

Dynamics of endoergic substitution reactions. I. Br+chlorinated aromatic compounds

Gary N. Robinson, Robert E. Continetti, and Yuan T. Lee

Citation: *The Journal of Chemical Physics* **89**, 6226 (1988); doi: 10.1063/1.455439

View online: <http://dx.doi.org/10.1063/1.455439>

View Table of Contents: <http://scitation.aip.org/content/aip/journal/jcp/89/10?ver=pdfcov>

Published by the [AIP Publishing](#)

Articles you may be interested in

[Reactions of substituted aromatic hydrocarbons with the Si\(001\) surface](#)

J. Vac. Sci. Technol. A **18**, 1965 (2000); 10.1116/1.582455

[Dynamics of endoergic substitution reactions. II. Br+{C₂H₂Cl₂}→Cl+{C₂H₂ClBr}](#)

J. Chem. Phys. **89**, 6238 (1988); 10.1063/1.455440

[Kerr Effect in Substituted Aromatic Nitro Compounds](#)

J. Appl. Phys. **41**, 2576 (1970); 10.1063/1.1659266

[Reactions of the Triplet States of Some Aromatic Compounds](#)

J. Chem. Phys. **41**, 2386 (1964); 10.1063/1.1726275

[The Influence of Aromatic Substitution on the C–Br Bond Dissociation Energy](#)

J. Chem. Phys. **19**, 657 (1951); 10.1063/1.1748313



Dynamics of endoergic substitution reactions. I. Br + chlorinated aromatic compounds

Gary N. Robinson,^{a)} Robert E. Continetti, and Yuan T. Lee

Materials and Chemical Sciences Division, Lawrence Berkeley Laboratory and Department of Chemistry, University of California, Berkeley, California 94720

(Received 7 July 1988; accepted 5 August 1988)

The endoergic substitution reactions $\text{Br} + \text{R-Cl} \rightarrow \text{Cl} + \text{R-Br}$ ($\text{R} = o-, m-, \text{ and } p\text{-CH}_3\text{C}_6\text{H}_4, \text{C}_6\text{H}_5, \text{C}_6\text{F}_5$; $\Delta H^\circ \approx 15 \text{ kcal/mol}$) have been studied using the crossed molecular beams method in the collision energy (E_c) range 20–35 kcal/mol. The $\text{CH}_3\text{C}_6\text{H}_4\text{Br}$ and $\text{C}_6\text{F}_5\text{Br}$ products were found to be mostly forward scattered with respect to the incident Br beam indicating that the lifetimes of the Br–R–Cl collision complexes are short compared to their rotational periods. The product translational energy distributions and excitation functions for these reactions are well reproduced by statistical calculations that assume that only a few vibrational modes in the collision complexes participate in intramolecular energy redistribution prior to Cl elimination. Ring substituents are found to affect both the extent of energy redistribution in the complexes and the probability of Br addition. For example, no substitution product was observed with $m\text{-CH}_3\text{C}_6\text{H}_4\text{Cl}$ or $\text{C}_6\text{H}_5\text{Cl}$. The relative magnitudes of the cross sections are explained in terms of possible features of the potential energy surfaces along their reaction coordinates.

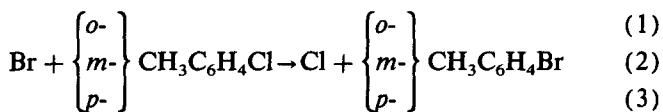
I. INTRODUCTION

Although homolytic, or free-radical, aromatic substitution reactions have been the subject of many kinetic studies,¹ their detailed dynamics in both the liquid and gas phases are only partially understood. In the gas phase, they proceed by addition of an atom or radical to an aromatic ring to form an activated cyclohexadienyl radical (collision complex) which subsequently decomposes through emission of another atom or radical. Previous crossed molecular beam studies of aromatic substitution reactions in this laboratory were directed towards determining (1) the extent of intramolecular vibrational energy redistribution in collision complexes of F atoms and substituted benzene molecules,² (2) the primary products of the reactions of O atoms with benzene and toluene,³ and (3) the energetics of halogen atom elimination from chemically activated haloxy-cyclohexadienyl radicals.⁴ All of the reactions studied were exoergic.

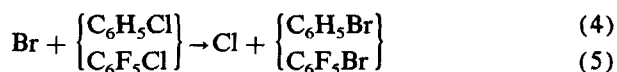
In this study, we have focused our attention on endoergic aromatic substitution reactions since elimination of the more strongly bound substituent is not the statistically favored mode of decay of a chemically activated radical. In addition, the cross sections for endoergic reactions typically display a strong positive dependence on collision energy. Thus, by studying the translational energy dependence of the reaction cross section as well as the product angular and translational energy distributions for the endoergic channel, we may gain some insight into the dynamical factors governing the formation and decomposition of chemically activated aromatic radicals. In this respect, the effect of ring substituents on both the probability of atomic addition and the degree of vibrational energy redistribution prior to bond fission are of particular interest.

^{a)} Present address: Department of Chemistry, Princeton University, Princeton, NJ.

We have carried out crossed molecular beam studies of the substitution reactions,



in the collision energy E_c range 20–30 kcal/mol and,



in the range 20–35 kcal/mol (Fig. 1). The results of these experiments shed new light on the way in which substituents influence the dynamics of aromatic substitution reactions. We have previously reported preliminary results for reactions (1)–(3)⁵; as discussed in Sec. III, our final analysis in this paper differs somewhat from that in Ref. 5(a). In the following paper^{4a} we discuss related studies on the reactions of Br with isomers of dichloroethylene.

II. EXPERIMENTAL

The crossed beam apparatus used in these experiments has been described previously.^{6,7} Two seeded, differentially pumped reagent beams were crossed at 90° in a vacuum chamber held at approximately 10^{-7} Torr. The products are detected with a triply differentially pumped mass spectrometric detector that rotates in the plane of the two beams.

The bromine atom beam was generated by passing a mixture of Br_2 in rare gas through a resistively heated high density graphite oven designed in this laboratory by Valentini *et al.*⁸ The Br_2 /rare gas mixture is created by bubbling approximately 700 Torr of He, Ne, or Ar through liquid bromine (reagent grade Fischer or Mallinckrodt) at 0 °C (vapor pressure, $vp = 60$ Torr). The oven had a nozzle diameter of 0.14 mm and was run at approximately 1400 °C. A conical graphite skimmer having an orifice diameter of 0.10

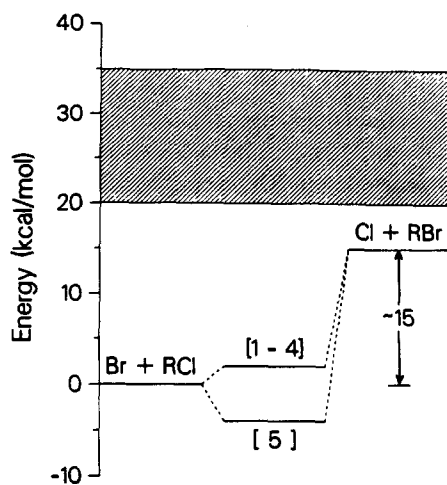


FIG. 1. Generalized reaction coordinate diagram. Shaded region indicates approximate collision energy range. Numbers represent the five reactions studied.

cm was positioned 0.76 cm from the nozzle. 90% of the Br_2 dissociated into Br atoms, as determined from a direct measurement of $[\text{Br}]/[\text{Br}_2]$ in the beam.

The chlorinated aromatic (R-Cl) molecular beam was formed by bubbling He through the liquid reagent held at a constant temperature in a bath and expanding the resulting mixture through a 0.21 mm diameter nozzle. Conditions were as follows: 450 Torr of He with *o*-, *m*-, or *p*-chlorotoluene (*o*-, *m*-, *p*-CT) at 60 °C ($v_p \approx 22$ Torr); 450 Torr He with pentafluorochlorobenzene (PFCB) at 19 °C ($v_p \approx 11$ Torr⁹); 350 Torr of He with chlorobenzene (CB) at 19 °C ($v_p = 9$ Torr¹⁰). A stainless steel skimmer with an orifice diameter of 0.66 mm was positioned 0.9 cm from the nozzle.

The source and gas feed line were heated with coaxial heating wire to a temperature of 200 °C for the CT experiments; the source temperature for the PFCB and CB experiments was 40 °C. *o*- and *p*-CT were purchased from MCB, *m*-CT from Aldrich, PFCB from Fairfield, and CB from Burdick and Johnson. All of the compounds were used without further purification, except for the *p*-CT which was distilled on a spinning band column.

A liquid nitrogen cooled copper cold finger was placed against the differential wall inside of the scattering chamber so that the detector would always face a cold surface during the angular scans thereby reducing the detector background at the product mass. Product angular distributions were measured by modulating the R-Cl beam with a 150 Hz tuning fork chopper and collecting data with the beam on and off using a dual channel scaler. Data were collected for 6–12 min per angle.

In order to compute relative cross sections for a given reaction at different collision energies, we scaled the product number density by the wide angle Br elastic scattering signals. Since the wide angle Br elastic scattering cross section does not change drastically as a function of energy, measuring Br on R-Cl elastic scattering allowed us to measure changes in the quantity $n_{\text{Br}} n_{\text{RCl}} v_{\text{rel}}$, where n_i = number density of beam *i* and v_{rel} = relative velocity. During each scan, the $m/e = 79$ signal was monitored at three different LAB angles. The angles were all beyond the maximum LAB angle for elastic scattering of Br on He so the Br^+ signal observed was from Br scattering on R-Cl. The contribution of undissociated Br_2 to the $m/e = 79$ signal was very small and was neglected. Relative values for $n_{\text{Br}} n_{\text{RCl}} v_{\text{rel}}$ derived from the Br elastic scattering signal at an angle of 16° are given in Table I.

The velocities of the reactant beams were measured using the time-of-flight (TOF) technique. A 256 channel scal-

TABLE I. Relevant experimental quantities for reactions (1)–(3).

Reaction	E_c^a	$\langle E'/E_{\text{av1}} \rangle^b$	$n_{\text{Br}} n_{\text{RCl}} v_{\text{rel}}^c$	p^d	B^d
Br/He } Br/Ne } + <i>o</i> -CT Br/Ar }	31	0.27	1.00	0.033	0.06
	25	0.27	0.54	0.035	0.03
	21	0.30	0.44	0.20	0.00
Br/He + <i>m</i> -CT	29	...	e		
Br/He } Br/Ne } + <i>p</i> -CT Br/Ar }	31	0.30	0.98	0.23	0.02
	25	0.30	0.59	0.21	0.00
	21	0.33	0.53	0.41	-0.01

^a All energies are in kcal/mol; collision energies reflect cross section weighting.

^b Fraction for most-probable collision energy.

^c Arbitrary units.

^d $P(E')$ parameters; $q = 1.85$.

^e The *m*-CT reaction was studied several weeks after the *o*- and *p*-CT experiments were completed. The Br/He + *o*-CT angular distribution was remeasured at this time, however. The *o*-BT and Br elastic signal levels indicated that the Br beam intensity was $\approx 50\%$ lower than during the earlier experiments; the *o*-BT signal-to-noise ratio had dropped by 20%. However, given the presence of elastic scattering background in the *m*-CT experiment (≈ 2 Hz at 46°), it is doubtful that we would have been able to see the signal even if the Br beam were twice as intense.

er interfaced with an LSI-11 computer accumulated the data. No TOF measurement was made for the *m*-CT beam, but its velocity should be identical to that of *o*-CT since both have the same vapor pressure [22 Torr; $v_p(p\text{-CT}) = 21$ Torr¹⁰] at 60 °C. The velocity of the CB beam was not measured under the exact conditions of the scattering experiment but was inferred from measurements at a slightly different nozzle and bath temperature. The peak laboratory beam velocities (in units of 10⁵ cm/s) v_{pk} , and speed ratios S_r ,¹¹ were: Br/He: $v_{pk} = 1.85$, $S = 6.1$; Br/Ne: $v_{pk} = 1.55$, $S = 6.9$; Br/Ar: $v_{pk} = 1.29$, $S = 8.4$; *o*-CT/He: $v_{pk} = 1.33$, $S = 11.3$; *p*-CT/He: $v_{pk} = 1.35$, $S = 11.8$; PFCB/He: $v_{pk} = 1.06$, $S = 14.8$; CB/He: $v_{pk} \approx 1.4$, $S \approx 15$. Product TOF spectra were measured using the cross-correlation method.⁷ A Cu-Be alloy wheel photoetched with a pseudorandom sequence of 255 open and closed slots was spun at 392 Hz giving 10 μ s/channel resolution in the TOF spectra. The flight path from wheel to ionizer was 30.0 cm. Counting times were approximately 1 h per angle for the Br + CT experiments and 2 h per angle for the Br + PFCB experiment.

III. RESULTS AND ANALYSIS

The product angular distributions and TOF spectra were fit using a forward convolution program¹² that starts with a separable form for the center-of-mass (c.m.) reference frame product flux distribution, $I_{c.m.}(\theta, E', E_c) = T(\theta)P(E', E_c)S_r(E_c)$, and generates a LAB frame angular distribution and TOF spectra averaged over the spread in relative velocity and the apparatus resolution. $T(\theta)$, the c.m. frame angular distribution, is taken to be a sum of three Legendre polynomials whose coefficients are varied to optimize the fit. A RRK functional form is used for $P(E')$, the c.m. frame product translational energy distribution:

$$P(E') = (E' - B)^p (E_{av1} - E')^q, \quad (6)$$

where B is related to any barrier in the exit channel and E_{av1} is the total energy available to the products ($E_c - \Delta H_0^\ddagger$). ΔH_0^\ddagger was taken to be 15 kcal/mol for all of the reactions studied (see Sec. IV). The parameters p , q , and B were optimized to give the best fit to the data (see Tables I and II).

$S_r(E_c)$ represents the collision energy dependence of the relative reaction cross section, i.e., the excitation function. For a given experiment, the spread in beam velocities and intersection angles gives rise to a spread in relative velocities and hence in collision energies. $\Delta E_c/E_c$ (FWHM) $\approx 30\%$ for the reactions with Br seeded in He and

$\approx 25\%$ for the reactions with Br seeded in Ne and Ar. Each beam velocity and intersection angle permutation corresponds to a different kinematic configuration (Newton diagram) over which the calculated angular distribution and TOF fits must be averaged. The collision energies corresponding to the most probable kinematic configurations are listed in Table I. Since the cross section is found to depend on collision energy, each kinematic configuration was weighted according to E_c using a function $S_r(E_c)$. Our method of weighting the Newton diagrams differs from that used in Ref. 5(a). Rather than using the calculated relative c.m. cross sections (which represent a convolution over the spread in relative velocity) and interpolating linearly between these values, the Newton diagrams were weighted with a multiple-point excitation function which was modified to fit the relative ratios of the LAB angular distributions at the different nominal collision energies.

The original form of $S_r(E_c)$ was derived from a statistical calculation of the product branching ratio as a function of energy (see Sec. IV). At each most-probable collision energy, the laboratory angular distribution calculated from the input $I(\Theta, E', E_c)$, $N_{calc}(\Theta)$, is scaled to the experimental angular distribution, $N_{exp}(\Theta)$, using a least-squares fit, i.e.,

$$\frac{d}{dz} \sum_i [N_{exp}(\Theta_i) - zN_{calc}(\Theta_i)]^2 = 0. \quad (7)$$

The input $S_r(E_c)$ is then modified so that the least-squares scaling parameters z , agree to within 1.5% indicating that the derived excitation function fits the experimental data. For reactions (1) and (3) the z parameters at the six most-probable collision energies (three for each reaction) agree with each other.

Since, for an endoergic reaction, the maximum translational energy of the products will depend strongly on E_c , a $P(E')$ with a unique value of E_{av1} was used for each Newton diagram in the analysis. Our present analysis procedure differs again from that used in Ref. 5(a) in that each $P(E')$ is normalized to its own area as opposed to being normalized to the area of the most-probable $P(E')$. This more favorable approach has the effect of enhancing the contribution of slow recoil velocity products to the calculated angular distributions and TOF spectra. The best-fit c.m. angular and energy distributions for the CT experiments are consequently somewhat different from those reported earlier, the main difference being that the $T(\theta)$ distributions here are more forward peaked.

TABLE II. Relevant experimental quantities for reactions (4) and (5).^{a,b}

Reaction	E_c	$\langle E'/E_{av1} \rangle$	$n_{Br} n_{RCl} v_{rel}$	p	B
Br/He + CB	30	...	1.29
Br/He	35	0.18	1.00	-0.10	0.08
Br/Ne } + PFCB	25	0.21	0.68	0.050	0.1
Br/Ar }	20	...	0.50

^a These experiments were carried out with a different inductor circuit, or "high-Q head," on the quadrupole mass filter than were the CT experiments so the transmission function of the mass spectrometer was different.

^b See legend to Table I; $q = 3.20$ for these fits.

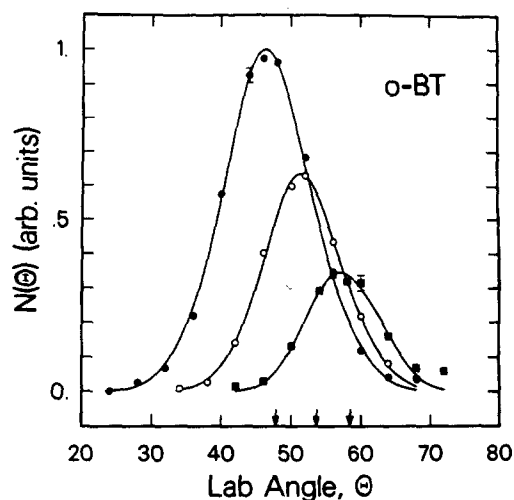


FIG. 2. *o*-BT ($m/e = 170$) laboratory angular distributions. ●: $E_c = 31$ kcal/mol; ○: $E_c = 25$ kcal/mol; ■: $E_c = 21$ kcal/mol. Signal is normalized to constant reactant flux but peak of $E_c = 31$ distribution is scaled to unity. Br beam is at 0° . Solid lines are fits to data using c.m. distributions in Figs. 7 and 8 and excitation function in Fig. 10. Error bars represent 90% confidence limits. Arrows indicate positions of center-of-mass angles with collision energy decreasing from left to right.

A. Br + *o*-, *m*-, *p*-CT

The ortho- and para-bromotoluene (BT) substitution products were detected at $m/e = 170$ (^{79}Br), however, the quadrupole mass spectrometer resolution was set sufficiently low to allow some of the ^{81}Br product to be detected as well. The product angular distributions are shown in Figs. 2 and 3. Elastic and inelastic scattering of impurity in the *p*-CT beam contributed to background at $m/e = 170$ near that beam. This was most problematic at $E_c = 21$ kcal/mol where the product signal level was lowest. At this energy the in/elastic scattering background was measured by substituting a properly diluted beam of Kr in Ar for the Br in Ar

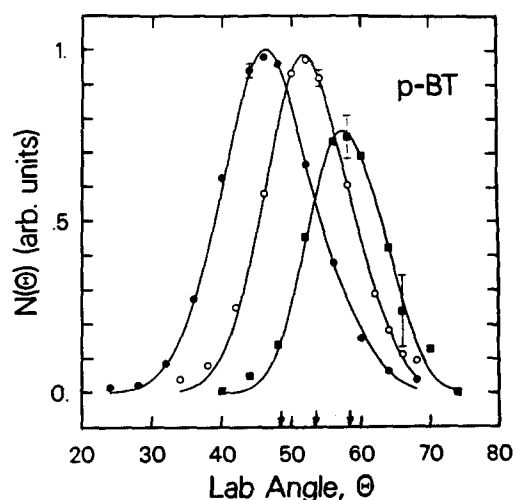


FIG. 3. *p*-BT ($m/e = 170$) laboratory angular distributions. See Fig. 2.

beam. It was then scaled to the product angular distribution at 74° and subtracted from it. At the peak of the $E_c = 31$ kcal/mol *o*-BT angular distribution, the product count rate was 20 Hz. The angular distributions reveal that, at all energies, the *o* and *p* products are mostly forward scattered with respect to the center-of-mass angle. Remarkably, no BT product was detected from Br + *m*-CT at a collision energy as high as 29 kcal/mol. TOF spectra of *p*-BT and of *o*-BT are presented in Figs. 4–6. At each collision energy, the peak product velocities are close to the center-of-mass velocity ($v_{c.m.}$, Fig. 9), indicating that little energy on the average is channeled into product translation.

The best fits to the data were obtained with $T(\theta)$ distributions that peak at 0° and 180° with maxima at 0° (Fig. 7). There is a range of acceptable values for the $P(E')$ parameters (as there is for the coefficients of the Legendre polynomials that constitute $T(\theta)$) yet the average fraction of energy that goes into product translation, $\langle E'/E_{av} \rangle$ (Table I), does not vary much within this range. Since the fits were relatively insensitive to the q parameter, which governs the curvature of the tail of the $P(E')$, this parameter was fixed for all the fits and the other parameters optimized. A value of 1.85 was chosen for q ; it was possible, however, to fit the data by raising q to 3.2 and varying p and B . The $q = 3.2$ distributions fall more steeply and consequently peak at higher energies than the $q = 1.85$ distributions. The $q = 1.85$ distributions (Fig. 8) peak between 0.0–2.0 kcal/mol, with the *o*-BT distributions peaking at lower energies and having slightly

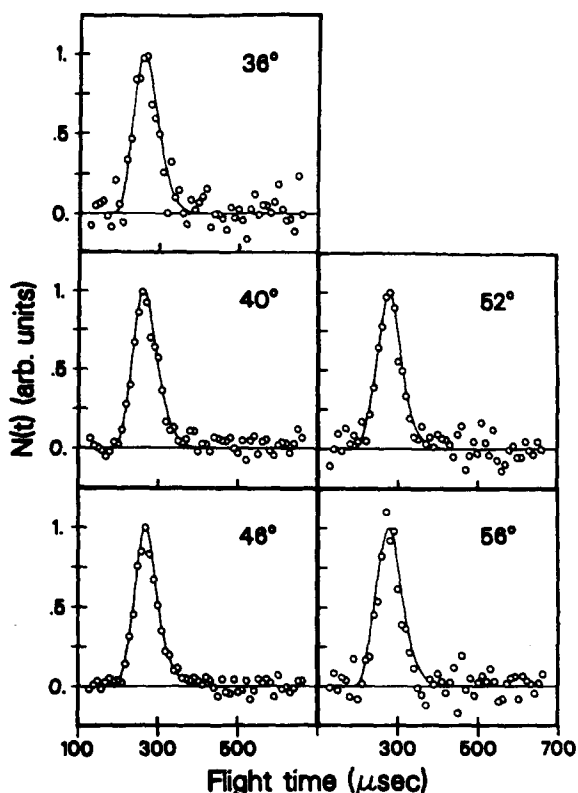


FIG. 4. *p*-BT ($m/e = 170$) time-of-flight spectra at $E_c = 31$ kcal/mol at five laboratory angles. Solid lines represent fits to data using c.m. distributions in Figs. 7 and 8 and excitation function in Fig. 10.

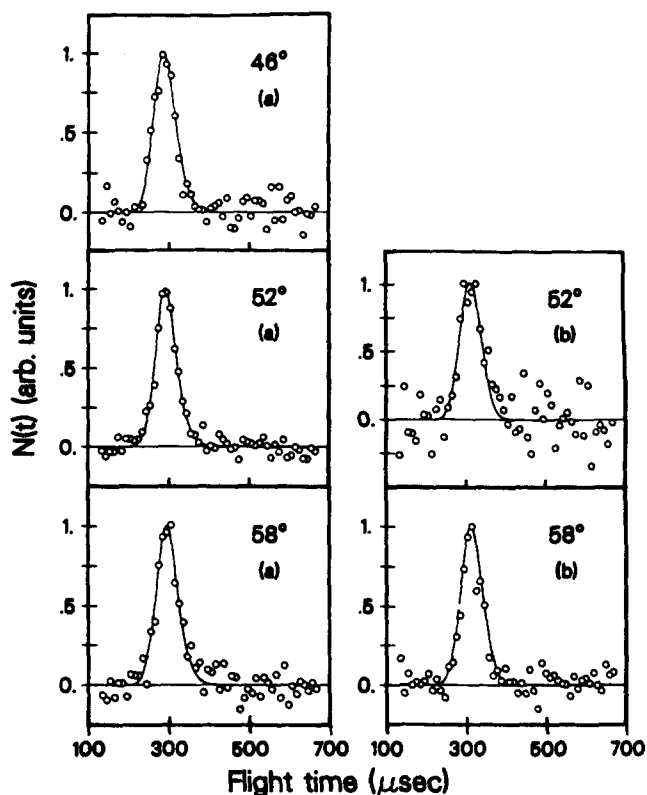


FIG. 5. *p*-BT ($m/e = 170$) time-of-flight spectra. (a) $E_c = 25$ kcal/mol; (b) $E_c = 21$. See Fig. 4.

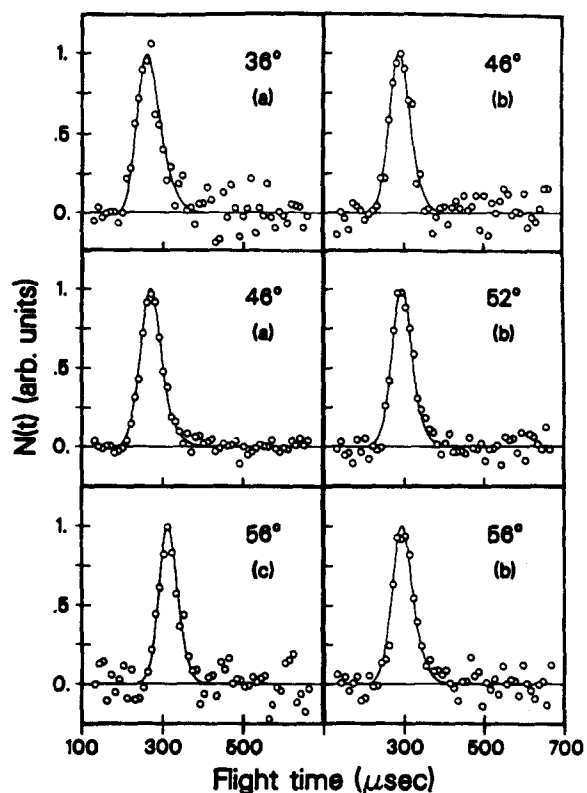


FIG. 6. *o*-BT ($m/e = 170$) time-of-flight spectra. (a) $E_c = 31$ kcal/mol; (b) $E_c = 25$; (c) $E_c = 21$. See Fig. 4.

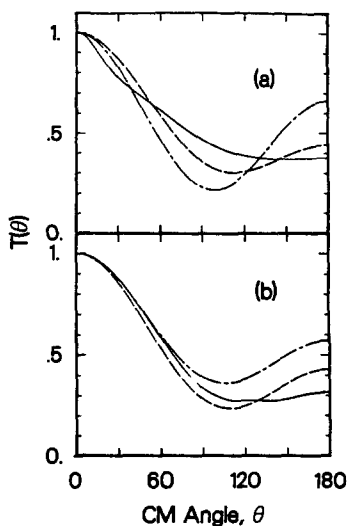


FIG. 7. Center-of-mass frame product angular distributions used in fits. (a) *o*-BT; (b) *p*-BT. — $E_c = 31$ kcal/mol; - - $E_c = 25$; - · - $E_c = 21$.

lower values of $\langle E'/E_{av1} \rangle$ than those for *p*-BT. For both reactions, $\langle E'/E_{av1} \rangle \approx 0.3$ at all collision energies. The following changes in the best-fit $P(E')$ for reaction (3), $E_c = 31$ kcal/mol, while not significantly affecting the fit, produced the indicated changes in $\langle E' \rangle$: $\pm 13\%$ in *p* parameter (equivalent to a change of $\pm 9\%$ in peak position), $\pm 2\%$ in $\langle E' \rangle$; ± 1 kcal/mol in ΔH_0^\ddagger , $\pm 6\%$ in $\langle E' \rangle$. A c.m. frame prod-

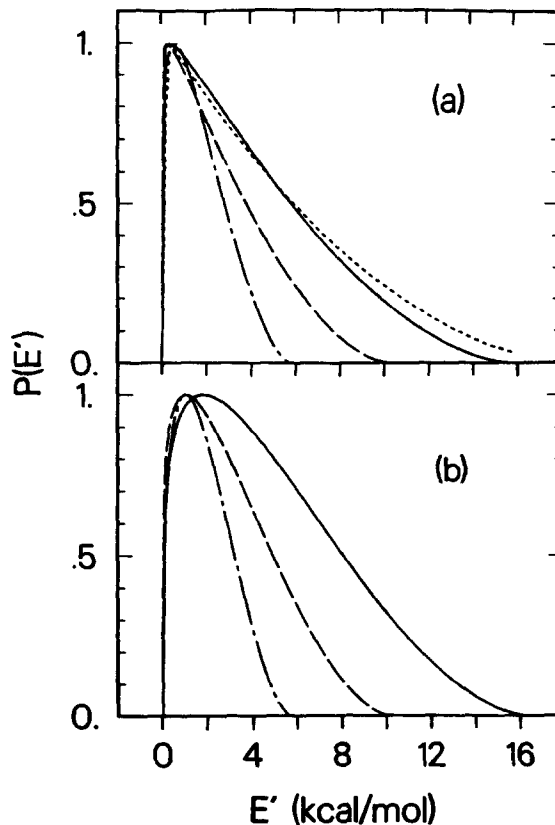


FIG. 8. Center-of-mass product translational energy distributions used in fits. (a) Br + *o*-CT: — $E_c = 31$ kcal/mol; - - $E_c = 25$; - · - $E_c = 21$; - · · - four-mode RRKM-AM calculation. (b) Br + *p*-CT: same as (a).

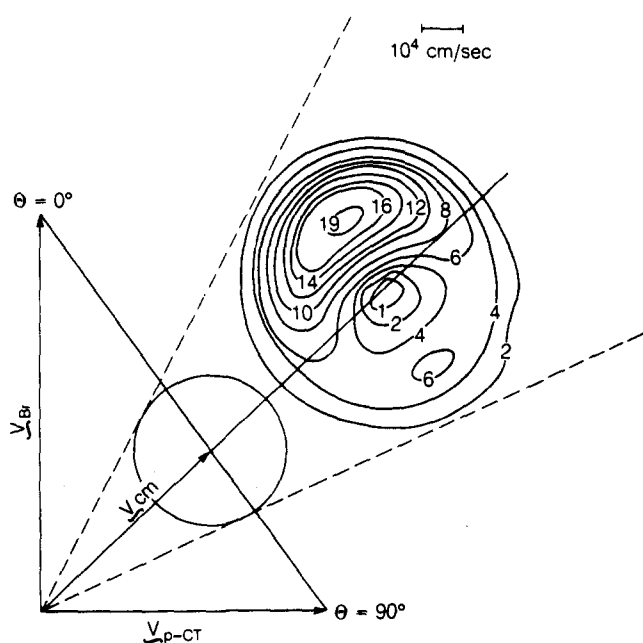


FIG. 9. Center-of-mass frame product flux contour diagram for reaction (3), $E_c = 31$ kcal/mol. Scale is for contours; scale for kinematic ("Newton") diagram is half of contour scale.

uct flux contour diagram for $\text{Br} + p\text{-CT} \rightarrow \text{Cl} + p\text{-BT}$, $E_c = 31$ kcal/mol, is given in Fig. 9. The overall quality of the fits justifies our use of a separable form for the c.m. flux distribution.

Since we have data at only three nominal collision energies for reactions (1) and (3), it is difficult to determine the exact form of the excitation functions. Excitation functions which reproduced the relative intensities of the laboratory angular distributions for reactions (1) and (3) are plotted in Fig. 10. We obtained equally good fits from excitation functions with thresholds at 18 and 17 kcal/mol for reactions (1) and (3), respectively. However, these functions change slope abruptly near $E_c = 20$ kcal/mol and are unlikely to be accurate representations of the true S_r . Because the collision energies for the Br/He, Br/Ne, and Br/Ar experiments overlap, the data constrain the curvature of S_r most strongly in the range $20 < E_c < 30$ kcal/mol. The curves extend to the maximum collision energy of the $E_c = 31$ kcal/mol experiments (≈ 44 kcal/mol); the shaded regions represent the uncertainty in S_r above 32 kcal/mol. Curves going through these regions yield values of z at $E_c = 31$ kcal/mol that are within 1.5% of \bar{z} for reactions (1) and (3) (where \bar{z} is determined from the fits based on the curves in Fig. 10). A change of $\pm 13\%$ in the p parameter of the $P(E')$ for reaction (3), $E_c = 31$ kcal/mol, changes z by $\pm 3\%$. These excitation functions will be discussed more in the next section.

The asymmetric c.m. angular distributions that we obtain indicate that the majority of 6-bromo-6-chloro-(3 or 5)-methyl-cyclohexadienyl (BCMC) complexes decompose in a time less than one rotational period.^{13(b)} The $p\text{-BT}$ c.m. angular distributions show more forward-backward symmetry at lower collision energies, suggesting that the lifetime of the $p\text{-BCMC}$ ¹⁴ complex increases relative to its rotational

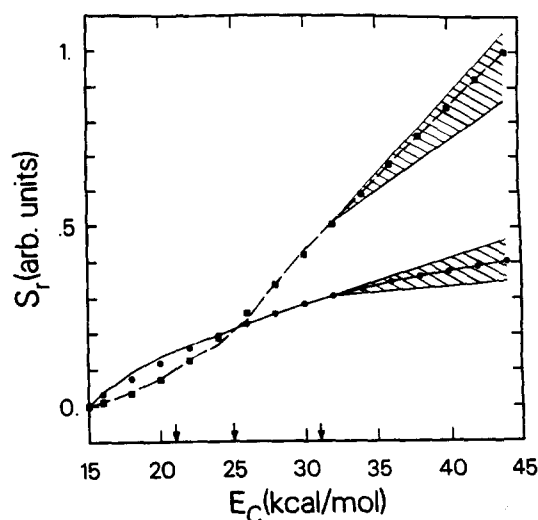


FIG. 10. Excitation functions for reactions (1) (---) and (3) (—). Arrows indicate most-probable experimental collision energies. Shaded regions indicate uncertainty in S_r above the highest most-probable collision energy. ■: six-mode RRKM branching ratio calculation; ●: three-mode RRKM calculation.

period as E_c decreases. We can estimate the rotational period of the $p\text{-BCMC}$ complex by assuming, for the sake of simplicity, that the Br atom collides perpendicular to the ring with an impact parameter of 0.9 \AA (the distance from the center of mass of $p\text{-CT}$ to the chlorinated carbon) and that the rotational angular momentum of the reagent is negligible. For the collision of Br with $p\text{-CT}$, $E_c = 31$ kcal/mol, the orbital angular momentum L will be $\approx 160\hbar$. The moment of inertia about the rotation axis of the complex is $\approx 880 \text{ amu} \cdot \text{\AA}^2$, assuming that the halogenated carbon is tetrahedral, that the C-Br and C-Cl bond lengths are 2.0 and 1.7 \AA , respectively, and that the ring is undistorted. The rotational period, given by $\tau_{\text{rot}} = 2\pi I/L$, will therefore be ≈ 5 ps in the present example. At a collision energy of 21 kcal/mol, $\tau_{\text{rot}} \approx 7$ ps.

The approximate product orbital angular momentum L' for reaction (3) at $E_c = 31$ kcal/mol, using a relative velocity corresponding to $\langle E' \rangle = 5$ kcal/mol and an exit impact parameter of 0.1 \AA (the distance between the chlorinated carbon and the center of mass of the complex, with the C-Cl bond perpendicular to the ring and the C-Br bond in the plane of the ring), is $\approx 6\hbar$, far lower than the initial $160\hbar$. It would take an average exit impact parameter of $\approx 2.7 \text{ \AA}$ for the total angular momentum of the complex to be carried away as product orbital angular momentum. However, even if most of the angular momentum of the collision were carried away in rotation of the BT product, the rotational energy of the product would be small (only ≈ 1.5 kcal/mol for $p\text{-BT}$ in the present example) because of its large moment of inertia ($I \approx 770 \text{ amu} \cdot \text{\AA}^2$).

The lack of a strong correlation between L and L' is the reason for the c.m. angular distributions not peaking more strongly in the forward and backward directions.^{13(a)} The larger amount of sideways scattering for $o\text{-BT}$ at 31.0 kcal/mol could indicate an even weaker L to L' correlation in

reaction (1) at high collision energies. This may be due to the more complicated rotational motion of the *o*-BCMC complex that results from both the asymmetry of the complex and, perhaps, a decreased steric barrier for Br addition to *o*-CT at higher collision energies.

A small fraction of the translational energy of BT will come from rotation of the complex at its exit transition state (TS). In the absence of extensive vibration-rotation coupling in the complex, the total rotational energy at this TS will be only ≈ 1.2 kcal/mol for *p*-BCMC ($E_c = 31$ kcal/mol, C-Cl bond perpendicular to the ring with a bond length of 2.6 \AA^{15}). The rotational motion of *o*-BCMC will, as noted above, be more complex. But the fact that the *o*-BT $P(E')$ distributions peak at slightly lower energies than those for *p*-BT could indicate that the ortho complex has a lower rotational energy at its exit TS than the para complex.

B. Br + CB, PFCB

As for the CT reactions, the substitution product from Br + PFCB, pentafluorobromobenzene (PFBB), $m/e = 246$, is mostly forward scattered with respect to the incident Br beam (Fig. 11). Elastic and inelastic scattering of impurities in the PFCB beam contributed significantly to the $m/e = 246$ signal near that beam at all three collision energies studied. As noted above, this background was measured by substituting a beam of Kr for the Br beam. The in/elastic angular distributions were then scaled and subtracted from the reactive angular distributions. Uncertainties associated with this scaling and subtraction lead to the error bars in the angular distributions. At $E_c = 20$ kcal/mol, no reactive signal could be discerned above the in/elastic background.

PFBB product TOF spectra are presented in Fig. 12. At $E_c = 35$ kcal/mol, TOF spectra were measured at 52° and

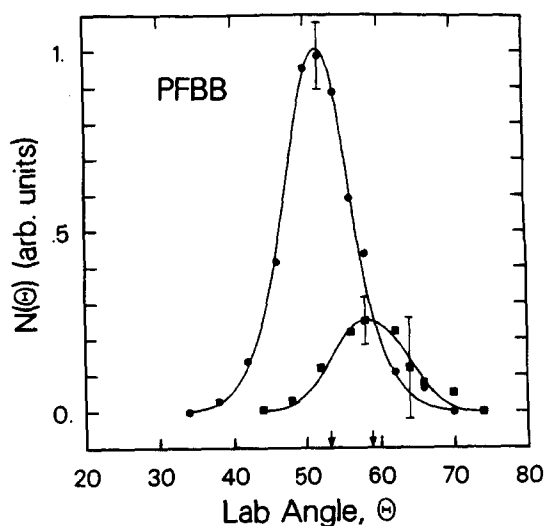


FIG. 11. PFBB ($m/e = 246$) laboratory angular distributions. \bullet : $E_c = 35$ kcal/mol; \blacksquare : $E_c = 25$ kcal/mol. Signal is normalized to constant reactant flux. Br beam is at 0° . Solid lines are fits to data using c.m. distributions in Figs. 13 and 14 and solid line excitation function in Fig. 15. Error bars represent 90% confidence limits.

62° . The signal-to-noise level at 62° was poor, making it difficult to distinguish the reactive and nonreactive components of the TOF spectrum. The narrowness of the angular distributions along with the relatively low $m/e = 246$ signal level (≈ 4 Hz at 52° at $E_c = 35$ kcal/mol) made it unprofitable to measure product TOF at several angles.

No bromobenzene (BB; $m/e = 156$) substitution signal was observed from Br + CB at a collision energy of 30 kcal/mol. There was a contribution from in/elastically scattered $^{79}\text{Br}_2$ to the $m/e = 156$ signal (≈ 9 Hz at $\Theta = 50^\circ$) at a mass spectrometer resolution equal to that at which the PFCB experiments were conducted. At a higher resolution no mass leakage occurred but at neither setting was any reactive signal observed. Our ability to observe PFBB product over BB is enhanced, however, by the larger mass of the former product which, assuming similar energy partitioning in reactions (4) and (5), causes its recoil velocity to be smaller. Since the transmission of the mass spectrometer changes with mass setting and the cracking patterns of the BB and PFBB products in the ionizer are not known, a quantitative comparison of the signal levels for the Br + CB and Br + PFCB reactions will not be attempted.

The uncertainties in the angular distribution data, especially at $E_c = 25$ kcal/mol, make it difficult to determine accurately the forms of the c.m. product distributions. An asymmetric, forward peaked $T(\theta)$ distribution is found to fit the $E_c = 35$ kcal/mol data (Fig. 13). At $E_c = 25$ kcal/mol, there is evidence of more backward scattered product. Again, this indicates that the lifetime of the adduct increases more than its rotational period as the collision energy is

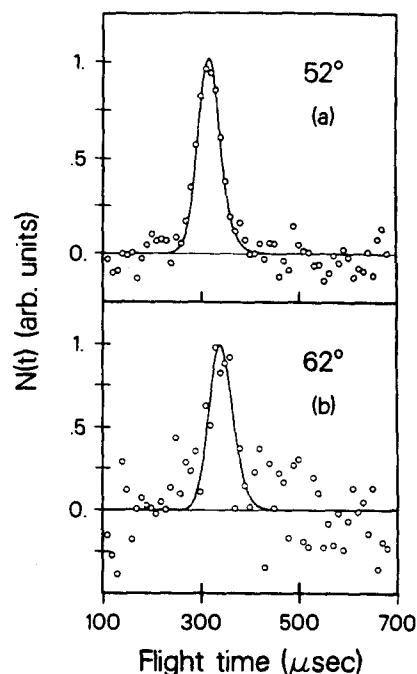


FIG. 12. PFBB ($m/e = 246$) time-of-flight spectra. (a) $E_c = 35$ kcal/mol; (b) $E_c = 25$ kcal/mol. Solid lines represent fits to data using c.m. distributions in Figs. 13 and 14 and solid line excitation function in Fig. 15.

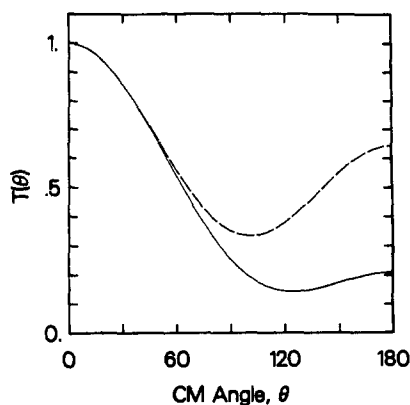


FIG. 13. Center-of-mass frame product angular distributions used in fits to PFBB data.— $E_c = 35$ kcal/mol; -- $E_c = 25$.

lowered. The $P(E')$ distributions (Fig. 14) are very narrow ($q = 3.2$), peaking slightly away from 0 kcal/mol. The data at both collision energies could also be fit with $P(E')$ distributions which sloped more gradually ($q = 1.8$) although the fits were not as good. $\langle E'/E_{av1} \rangle \approx 0.19$ for both of the $q = 3.2$ distributions (Table II) and 0.23 for the $q = 1.8$, $E_c = 35$ kcal/mol, distribution.

In the absence of a product angular distribution at $E_c = 20$ kcal/mol, it was possible to reproduce the ratio of the $E_c = 25$ and 35 kcal/mol angular distribution intensities with two different excitation functions, one of which has a threshold of 20 kcal/mol (Fig. 15). The average ratio of the relative cross sections at the two nominal collision energies, $\bar{S}_r(35)/\bar{S}_r(25)$, is 3.4 for the two excitation functions. The fits to the data that are presented were generated with the lower threshold curve. As for the CT reactions, the shaded region indicates the uncertainty in S_r above the highest nominal collision energy.

IV. DISCUSSION

A. Br + *o*-, *m*-, *p*-CT

The endoergicities of the isomeric CT reactions under study should not differ markedly from one another. The

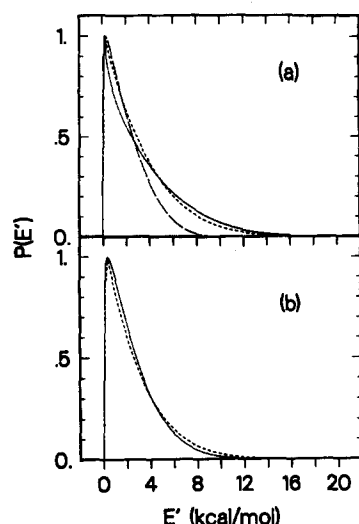


FIG. 14. Center-of-mass frame product translational energy distributions used in fits to PFBB data.

(a) — $E_c = 35$ kcal/mol ($q = 3.2$); -- $E_c = 25$ kcal/mol ($q = 3.2$); --- eight-mode RRKM-AM calculation; (b) — $E_c = 35$ kcal/mol ($q = 7.0$); - - - ten-mode RRKM-AM calculation.

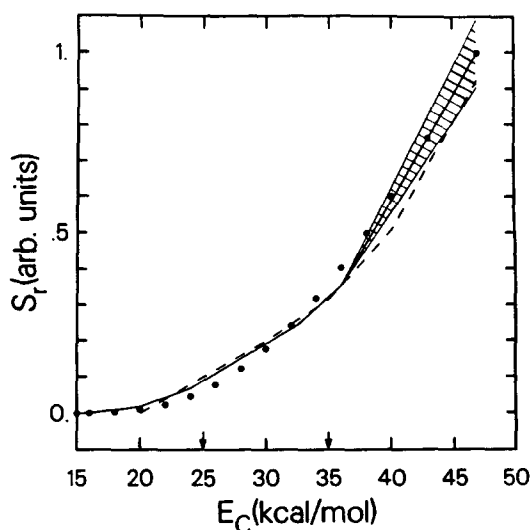


FIG. 15. Excitation functions for reaction (5). See Fig. 10.

●: ten-mode RRKM branching ratio calculation. The solid and dashed curves have different thresholds; see the text.

heats of formation of *o*-, *m*-, and *p*-CT [ΔH_{f298}° (g)] are 3.8, 4.1, and 5.3 kcal/mol, respectively.^{10,16} We were able to find heat of formation data for the para isomer of bromotoluene (BT) only [ΔH_{f298}° (g) = 13.0 kcal/mol^{10,17}], but Szwarc's work¹⁸ indicates that the C-Br bond dissociation energies in *o*-, *m*-, and *p*-BT differ by only 0.6 kcal/mol. Using the known values for ΔH_{f298}° of Br, Cl,¹⁹ *p*-CT, and *p*-BT, we calculate $\Delta H_{298}^\circ = 10.1$ kcal/mol for the reaction, $\text{Br} + p\text{-CT} \rightarrow p\text{-BT} + \text{Cl}$. This number strikes one as being too low considering that $\Delta H_{298}^\circ = 15$ kcal/mol for the reaction, $\text{Br} + \text{C}_6\text{H}_5\text{Cl} \rightarrow \text{C}_6\text{H}_5\text{Br} + \text{Cl}$.²⁰ In the absence of firm values for the heats of formation of the CT and BT isomers, we have used an endoergicity of 15 kcal/mol for the present reactions.

The energetics of Br addition to CT are, as far as we can tell, unknown. Ref. 21 gives $\Delta H_{298}^\circ = -8.8$ kcal/mol for $\text{Br} + \text{C}_2\text{H}_4 \rightarrow \text{C}_2\text{H}_4\text{Br}$. The exothermicity of Br addition to benzene ($\Delta H_{\text{add}}^\circ$) will reflect the loss in resonance stabilization energy (RSE) that results from the disruption of the π electron framework of the ring. In the case of H atom addition to benzene the loss in RSE will be approximately 11 kcal/mol.²² We conclude, therefore, that the BCMC radical will be unbound by ≈ 2 kcal/mol relative to reactants! Rodgers *et al.*²³ arrive at a similar value for the endothermicity of Br addition to benzotrifluoride. As a result, we do not expect there to be a potential minimum along the reaction coordinate corresponding to the BCMC complex and it is not surprising that substitution occurs in less than one rotational period.

Remarkably, very little of the energy available to the products ends up in translation. Apparently the vibrational modes of the aromatic ring act as a strong energy sink with Cl elimination occurring only when sufficient energy has accumulated in the C-Cl bond. Although a large fraction of the total available energy finds its way into BT product vibration, it does not seem that Cl elimination from BCMC is a statistical process involving energy sharing among all of the

vibrational degrees of freedom of the complex. We have calculated RRKM-AM $P(E')$ distributions^{24,25} for BT, $E_c = 31$ kcal/mol, assuming different numbers of active vibrational modes²⁶ with an endoergicity of 15 kcal/mol. The maximum centrifugal barrier B'_m is treated as a parameter. Since the activation energies for Cl addition reactions are known to be very near zero,²⁷ we have no reason to expect that there will be a barrier above the threshold for Cl elimination. Although a definitive comparison between the experimental and RRKM-AM $P(E')$ distributions is not possible given the uncertainties in the fits, we obtain reasonable agreement between the experimental *o*-BT $P(E')$, $E_c = 31$ kcal/mol, and a RRKM-AM $P(E')$ calculated assuming that four modes with frequencies in the range 700–800 cm^{-1} are active in energy redistribution and with $B'_m = 0.40$ kcal/mol and $\Delta H_0^\ddagger = 15$ kcal/mol (Fig. 8). If ΔH_0^\ddagger is taken to be 10 kcal/mol, comparable agreement is obtained with five active modes. Note that the q parameter determines the curvature of the experimental $P(E')$ which in turn reflects the number of active modes in the complex. Thus, the data seem to indicate that only a limited number of vibrational degrees of freedom participate in energy sharing prior to Cl elimination.

Such a mechanism is not unexpected. At collision energies not far from threshold, endoergic substitution reactions involving molecules with many vibrational degrees of freedom must occur in a quasidirect fashion since, as more vibrational modes participate in energy redistribution, the probability that the collision complex will decompose by eliminating the more strongly bound substituent drops relative to that of its decomposing to reactants. This is due to the fact that the probability of X elimination η_X is proportional to the density of states at the TS for X elimination. The smaller the number of active vibrational modes, the smaller the difference between the state densities for the exoergic and endoergic channels and the more Cl elimination will compete with Br elimination. For example, taking η_X to be the microcanonical RRKM rate constant for X elimination [classically, $\eta_X \propto (\epsilon^\ddagger/E^*)^{s-1}$, where ϵ^\ddagger is the excess energy, $E^* - E_0$, at the X elimination TS and s is the number of active vibrational modes²⁸], at $E_c = 30$ kcal/mol, $\eta_{\text{Br}}/\eta_{\text{Cl}} = 270$ with $s = 12$ ($\nu = 300\text{--}800$ cm^{-1}) whereas with $s = 4$, $\eta_{\text{Br}}/\eta_{\text{Cl}} = 6$.

In another check of the extent of intramolecular vibrational energy redistribution in BCMC, we measured the TOF of CT from the decay channel BCMC \rightarrow Br + CT near the center-of-mass angle, $\Theta_{\text{c.m.}}$ for reaction (3), $E_c = 21$ kcal/mol, and reaction (1), $E_c = 31$ kcal/mol. If energy redistribution in the BCMC complex were complete prior to unimolecular decay, the reactants formed from this channel would have very slow c.m. frame recoil velocities, i.e., their LAB velocities will be close to $v_{\text{c.m.}}$ (Fig. 9). In both cases, however, the TOF of in/elastically scattered CT near $\Theta_{\text{c.m.}}$ obtained by substituting Kr for Br was very similar to that obtained with Br. This suggests not only that the Br addition cross section is substantially smaller than the in/elastic scattering cross section but also that a “statistical” collision complex does not form. If η_{Br} were indeed two orders of magnitude larger than η_{Cl} (as one would predict from a 12-

mode RRKM calculation), we would have been able to see a substantial peak in the *o*-CT TOF spectrum at $E_c = 31$ kcal/mol corresponding to slow *o*-CT travelling at the velocity of the center of mass since the fast and slow components of the elastic scattering TOF spectrum were well resolved at this energy. Thus, our inability to observe slow *o*-CT provides additional (though indirect) evidence that only a few modes are active during the reaction.

Further support for a reduced mode mechanism comes from an examination of the excitation functions. The measured relative cross sections can be expressed as the product of the cross section for forming the BCMC adduct and the relative probability of decomposition of the adduct through Cl elimination,

$$S_r = \sigma_{\text{add}} [\eta_{\text{Cl}} / (\eta_{\text{Cl}} + \eta_{\text{Br}})]. \quad (8)$$

If intramolecular energy randomization were complete prior to atomic elimination, the quantity in brackets would be equivalent to the RRKM branching ratio S_{RRKM} . For an endoergic reaction, this quantity will be a strongly increasing function of energy. With the assumption that σ_{add} does not depend strongly on collision energy (see below), we initially used three- and six-mode S_{RRKM} functions to represent $S_{r,p\text{-BT}}$ and $S_{r,o\text{-BT}}$, respectively. These curves needed to be modified very little to fit the data. The three-mode ($\nu = 700\text{--}800$ cm^{-1}) and six-mode ($\nu = 700\text{--}900$ cm^{-1}) RRKM curves are plotted in point-form in Fig. 10 alongside the experimental excitation functions.

It is certainly plausible that the *o*-BCMC collision complex has a larger number of active vibrational modes than *p*-BCMC. We have already noted that the *o*-BT $P(E')$ distributions have slightly lower values of $\langle E'/E_{\text{avl}} \rangle$ than those for *p*-BT. The reduced symmetry of the *o*-BCMC complex may allow for enhanced vibrational energy redistribution through state mixing. Coupling of methyl group torsion to ring vibrations is believed to be responsible for accelerated IVR in S_1 *p*-fluorotoluene.^{29,30} Although the barrier to methyl torsion is likely to be higher in *o*-CT than in *p*-CT,³¹ the methyl group is closer to the collision site in the ortho isomer.

The normalization factor used to scale S_{RRKM} (six-mode) to $S_{r,o\text{-BT}}$ at $E_c = 44$ kcal/mol is ≈ 5 times that used to scale S_{RRKM} (three-mode) to $S_{r,p\text{-BT}}$ at the same energy. If the probability of C–Br bond formation is independent of collision energy, this suggests that σ_{add} (*o*-CT) is approximately five times larger than σ_{add} (*p*-CT). A larger addition cross section for *o*-CT can be rationalized along the above lines. The greater number of active modes in *o*-BCMC might serve to dissipate the energy of the collision better, allowing Br to add more readily to *o*-CT than to *p*-CT.

Two points should be made regarding the way in which we interpret our results. First, in saying that a product $P(E')$ or excitation function is reproduced well by a limited-mode RRKM calculation, we do not maintain that a small number of modes are in microcanonical equilibrium prior to bond rupture. In fact, IVR competes with bond rupture in the present reactions and RRKM theory cannot, in principle, be applied. The number of active modes is thus a relative measure of the extent of intramolecular energy transfer prior to

Cl elimination. Second, it seems rather tenuous to divide the substitution reaction into addition and decomposition steps when C–Br bond formation is endoergic and so few vibrational degrees of freedom participate in the reaction. However, both the moderate amount of backward scattering and the change in the effective number of modes as the substituents near the collision site are changed (see also Sec. IV B) indicate that these reactions proceed through (short-lived) collision complexes and that we may divide them into two steps for conceptual purposes.

In arriving at a value for the number of active vibrational modes in *o*-BCMC and *p*-BCMC, we assumed that the cross section for Br addition to *o*-CT and *p*-CT does not vary with E_c . However, the probability of C–Br bond formation might indeed depend on collision energy. In particular, steric blocking of the chlorinated carbon by the methyl group in *o*-CT might cause $\sigma_{\text{add}}(\textit{o}\text{-CT})$ to change more drastically with energy than $\sigma_{\text{add}}(\textit{p}\text{-CT})$. If the number of active modes in *o*-BCMC and *p*-BCMC were the same, the lower substitution cross section for reaction (1) below 25 kcal/mol could result from a narrowing of the acceptance angle of the Br + *o*-CT potential energy surface (PES) relative to that of the Br + *p*-CT PES. The range of approach geometries that can lead to reaction should grow with increasing energy; as noted in the previous section, the c.m. angular distributions for reaction (1) do suggest that the approach angle widens at higher E_c . With a greater number of low frequency modes in the vicinity of the collision, *o*-CT could therefore have a larger addition cross section than *p*-CT at collision energies above 25 kcal/mol. Thus, the excitation functions for Br addition to *o*-CT and *p*-CT may influence the forms of $S_{r,\textit{o}\text{-BT}}$ and $S_{r,\textit{p}\text{-BT}}$ and the steeper slope of $S_{r,\textit{o}\text{-BT}}$ need not necessarily be due to a larger number of active modes in *o*-BCMC than in *p*-BCMC.

Based on our experimental signal levels, the substitution cross section for *m*-CT at $E_c = 29$ kcal/mol is estimated to be at least a factor of 10 lower than for *o*-CT at 31 kcal/mol. It is well known that the methyl group is an ortho–para directing substituent in electrophilic (ionic and atomic) substitution reactions. This phenomenon is usually explained in terms of the electron donating capability of the methyl group,^{32,33} which stabilizes the *o*- and *p*- adducts by either increasing the *o*- and *p*- frontier electron populations in the reactant molecule or lowering the total π electron energy of the *o*- and *p*- adducts relative to the *m*- adduct.

There have been no rigorous quantum mechanical calculations of the heats of formation of the isomeric methyl cyclohexadienyl radicals (much less halogenated methyl cyclohexadienyl radicals such as BCMC). However, using a modified version of Hückel theory, Wheland³⁴ calculated the energy change associated with localizing an electron at the ortho, meta, and para positions of various aromatic molecules, thereby removing it from conjugation with the ring. Although this “localization” energy has traditionally been correlated with the activation energy for addition to a particular ring position, we may associate it with the thermodynamic stability of the resulting radical. For toluene, Wheland found a mere 0.8 kcal/mol difference between the *o*- and *m*- localization energies. Such small differences in thermo-

dynamic stability will not have an observable effect on the dynamics of aromatic substitution reactions at the collision energies of our experiments.

A possible explanation is that the reactivities of the isomers of CT are governed by the shape of the Br–CT PES along the reaction coordinate. The increased electron populations ortho and para to the methyl group in CT could enhance the long range attraction between Br and these sites, but such an attraction might not be strong at the experimental collision energies. The shape of the potential in the exit valley might be the key. Since the ΔH° are nearly the same for the three isomeric reactions, the ΔG° and K_{eq} for all three reactions will also be roughly the same. Therefore, the rates of the reverse reactions, $\text{Cl} + \textit{o}\text{-}, \textit{p}\text{-BT} \rightarrow \text{Br} + \textit{o}\text{-}, \textit{p}\text{-CT}$, must be accelerated relative to the rate of $\text{Cl} + \textit{m}\text{-BT} \rightarrow \text{Br} + \textit{m}\text{-CT}$. A longer range attraction between Cl and *o*- and *p*-BT, manifesting itself in a more gradually sloping potential in the reverse endoergic direction, might be responsible for such a rate enhancement. Alternatively, the lower π electron energies of the *o*- and *p*- complexes may cause the *o*- and *p*- surfaces to rise more gradually. In either case, translational energy will be better able to promote the endoergic reaction.

Classical trajectory studies on several different potential energy surfaces lend support to these ideas. Polanyi and co-workers³⁵ have observed that translational energy is favored over vibrational energy in endoergic reactions with a gradual ascent to the barrier crest. Likewise, Chapman³⁶ has found that the curvatures of the $\text{Be} + \text{HF} \rightarrow \text{BeF} + \text{H}$ and $\text{NO} + \text{O}_3 \rightarrow \text{NO}_2 + \text{O}_2$ surfaces have marked effects on the excitation functions and product energy distributions of these reactions. Of course, the slope of the PES will affect the translational energy dependence of the reaction cross section most when only a few vibrational modes participate in energy sharing prior to bond breakage and when reactant translational energy can couple directly into the bond breaking coordinate. Although the substitution reactions under study are not “direct,” they do seem to satisfy these criteria.

B. Br + CB, PFCB

As discussed in relation to the Br + CT reactions, Br addition to CB should be endoergic by ≈ 2 kcal/mol. However, because of the weakness of the π bond in fluorinated unsaturated molecules, Br addition to PFCB should be somewhat exoergic. From photodissociation experiments on several fluorinated bromo-iodoalkanes, Lee and co-workers have derived C–Br bond dissociation energies (D_0°) in $\text{CF}_2\text{CF}_2\text{Br}$ and CFHCFHBr of 20 and 12 kcal/mol, respectively.³⁷ Neglecting the effect of resonance stabilization, let us assume that $D^\circ(\text{C–Br}) = 15$ kcal/mol in the pentafluorochloro-bromo-cyclohexadienyl (PFCBC) radical. Therefore, a loss of 11 kcal/mol in resonance stabilization energy would make Br addition to PFCB exoergic by approximately 4 kcal/mol.

As we noted at the beginning of Sec. IV A, $\Delta H_{298}^\circ = 15$ kcal/mol for reaction (4). However, the overall endoergicity of reaction (5) is uncertain. Krech *et al.*³⁸ measured $\Delta H_{f298}^\circ(\text{C}_6\text{F}_5\text{Br}) = -170.1$ kcal/mol. With ΔH_{f298}°

(C₆F₅Cl) = -193.6 kcal/mol from experiment³⁹ and known heats of formation for Cl and Br,¹⁹ this gives $\Delta H_{298}^{\circ} = 25.8$ kcal/mol for reaction (5). From group additivity, $\Delta H_{f298}^{\circ}(\text{C}_6\text{F}_5\text{X}) = -197.8$ kcal/mol (X = Cl) and -183.3 (X = Br).⁴⁰ Together these yield $\Delta H_{298}^{\circ} = 16.8$ kcal/mol. With experimental values for the heats of formation of the products or reactants, these calculated $\Delta H_{f298}^{\circ}(\text{C}_6\text{F}_5\text{X})$ give $\Delta H_{298}^{\circ} = 30.0$ kcal/mol and 12.6 kcal/mol, respectively. Thus, lacking a firm value for the endoergicity of this reaction, we have assumed $\Delta H_0^{\circ} = 15$ kcal/mol.

Considering the larger number of low frequency vibrational modes in the fluorinated complex (C-F stretching, ≈ 1000 cm⁻¹, and C-C-F bending, ≈ 500 cm⁻¹), one might expect vibrational energy redistribution prior to bond cleavage to be more extensive in PFCBC than in BCMC. Indeed, the product translational energy distributions for reaction (5) suggest that this is the case.

The experimental $E_c = 35$ kcal/mol $P(E')$ plotted in Fig. 14(a) ($q = 3.2$) is in fair agreement with an eight-mode ($\nu = 440\text{--}650$ cm⁻¹) RRKM-AMP(E') ($B'_m = 0.20$ kcal/mol). If ΔH_0° is taken to be 20 kcal/mol, comparable agreement is obtained with six modes. Since it is possible to fit both the *o*-BT and PFBB data with $P(E')$'s having the same q parameter (e.g., $q = 3.2$), we cannot conclude just from the shapes of the product energy distributions in Figs. 8(a) and 14(a) that there are more active modes in PFCBC than in *o*-BCMC. However, the PFBB, $E_c = 35$ kcal/mol, data could be fit reasonably well with a $q = 7.0$ $P(E')$ [Fig. 14(b)] whereas the *o*-BT and *p*-BT data could not. This $P(E')$ agrees with a ten-mode ($\nu = 440\text{--}700$ cm⁻¹) RRKM-AMP(E') ($B'_m = 0.40$ kcal/mol). In addition, the average fraction of available energy in product translation is $\approx 10\%$ lower for reaction (1.5) than for reactions (1) and (3).

This is noteworthy in light of Quack's argument that an apparently nonstatistical $P(E')$ for a substitution reaction with a loose TS need not imply incomplete energy redistribution in the collision complex.⁴¹ He has been able to reproduce experimental $P(E')$ distributions for substitution reactions reasonably well by including an angular contribution to the interaction potential in the adiabatic channel model while assuming that all vibrational modes in the collision complex are active. However, the differences that we observe between the BT and PFBB $P(E')$ distributions point to more complete energy sharing in PFCBC than in BCMC prior to Cl elimination.

The slope of the PFBB excitation function also supports this view. The excitation function used to fit the PFBB data (solid curve in Fig. 15) was derived from a ten-mode RRKM branching ratio calculation, again assuming that the cross section for complex formation does not depend on collision energy in the range of our experiment. The experimental and RRKM curves agree reasonably well. The 20 kcal/mol threshold for the dashed curve suggests that our data are consistent with a higher endoergicity than 15 kcal/mol for reaction (5).

The marked difference in cross section between reactions (4) and (5) is likely to be due to differences in σ_{add} for the two reactions. As discussed above in relation to reactions

(1) and (3), Br should "stick" better to the molecule with the larger number of low frequency dissipative modes in the vicinity of the collision. The slight exoergicity of Br addition to PFCB will increase the density of dissipative states and render the Br-PFCB interaction more "attractive" than the Br-CB interaction. Considering that the probability of Cl elimination should be smaller for the complex with the larger number of active vibrational modes [i.e., $\eta_{\text{Cl}}/(\eta_{\text{Cl}} + \eta_{\text{Br}})$ decreases as the number of active modes increases, see Eq. (3)], $\sigma_{\text{add}}(5)/\sigma_{\text{add}}(4)$ will be greater than a simple comparison of the signal levels for the two reactions at comparable collision energies would suggest.

Halogen substituents are known to deactivate aromatic molecules to electrophilic attack but their ability to back-donate *p*-electrons to the ring makes them ortho-para directing.⁴² A CNDO study of fluorobenzene and *p*-difluorobenzene has shown increased π electron populations ortho and para to the F atoms.⁴³ It is not clear, however, whether π electron backbonding stabilizes PFCBC relative to bromochloro-cyclohexadienyl radical and thereby enhances the substitution cross section for Br + PFCB.

Finally, in comparing our results for reactions (1) and (3) with those for reaction (4), we note how strongly the methyl group enhances the cross section for Br addition to the ring. The features of the PES that are responsible for this large difference in cross section should be analogous to those responsible for the greater reactivity of *o*- and *p*-CT relative to *m*-CT.

V. CONCLUSIONS

A complex interplay of phenomena underlies our observations for these endoergic aromatic substitution reactions. Competition between intramolecular vibrational energy redistribution and Cl elimination results in asymmetric, forward peaked product c.m. angular distributions and translational energy distributions and excitation functions that can be modeled by assuming that a limited number of vibrational modes participate in energy sharing in the energized radicals. Ring substituents appear to affect the dynamics by influencing the probability of Br addition and the extent of energy redistribution in the radicals. The electronic effects responsible for the different reactivities of the CT isomers may manifest themselves in the slope of the potential energy surface along the reaction coordinate.

ACKNOWLEDGMENTS

We would like to thank Professor Sidney Benson, Professor A. Streitwieser, Dr. D. Golden, and Dr. G. Nathanson for helpful discussions. The technical assistance of A. Williamson is also appreciated. This work was supported by the Director, Office of Energy Research, Office of Basic Energy Sciences, Chemical Sciences Division of the U. S. Department of Energy under Contract No. DE-ACO3-76SF00098.

- ¹(a) G. H. Williams, *Homolytic Aromatic Substitution* (Pergamon, New York, 1960); (b) M. J. Perkins, in *Free Radicals*, edited by J. Kochi (Wiley, New York, 1973), Vol. 2, pp. 231–271; (c) J. March, *Advanced Organic Chemistry*, 3rd ed. (Wiley, New York, 1985), Chap. 14.
- ²K. Shobatake, J. M. Parson, Y. T. Lee, and S. A. Rice, *J. Chem. Phys.* **59**, 1427 (1973); K. Shobatake, Y. T. Lee, and S. A. Rice, *ibid.*, 1435 (1973).
- ³S. J. Sibener, R. J. Buss, P. Casavecchia, T. Hirooka, and Y. T. Lee, *J. Chem. Phys.* **72**, 4341 (1980); R. J. Baseman, R. J. Buss, P. Casavecchia, and Y. T. Lee, *J. Am. Chem. Soc.* **106**, 4108 (1984).
- ⁴R. J. Brudzynski, Ph. D. thesis, University of California, Berkeley, 1987.
- ⁵(a) G. N. Robinson, R. E. Continetti, and Y. T. Lee, *Faraday Discuss. Chem. Soc.* **84** (1987); (b) G. N. Robinson, Ph. D. thesis, University of California, Berkeley, 1987.
- ⁶Y. T. Lee, J. D. McDonald, P. R. LeBreton, and D. R. Herschbach, *Rev. Sci. Instrum.* **40**, 1402 (1969).
- ⁷R. K. Sparks, Ph. D. thesis, University of California, Berkeley, 1979.
- ⁸J. J. Valentini, M. J. Coggiola, and Y. T. Lee, *Rev. Sci. Instrum.* **48**, 58 (1977).
- ⁹J. D. Cox and G. Pilcher, *Thermochemistry of Organic and Organometallic Compounds* (Academic, New York, 1970).
- ¹⁰*CRC Handbook of Chemistry and Physics*, 64th ed. (CRC, Cleveland, 1983).
- ¹¹R. B. Bernstein, *Chemical Dynamics via Molecular Beam and Laser Techniques* (Oxford University, New York, 1982), p. 30.
- ¹²R. J. Buss, Ph. D. thesis, University of California, Berkeley, 1979.
- ¹³(a) W. B. Miller, S. A. Safron, and D. R. Herschbach, *Faraday Discuss. Chem. Soc.* **44**, 108 (1967); (b) G. A. Fisk, J. D. McDonald, and D. R. Herschbach, *ibid.* **44**, 228 (1967).
- ¹⁴Rather than use the formal nomenclature for the BCMC radicals, we identify them with a prefix corresponding to the aromatic reagent.
- ¹⁵H. B. Schlegel and C. Sosa, *J. Phys. Chem.* **88**, 1141 (1984).
- ¹⁶D. R. Stull, E. F. Westrum, Jr., and G. C. Sinke, *The Chemical Thermodynamics of Organic Compounds* (Wiley, New York, 1969).
- ¹⁷T. Holm, *J. Organometal. Chem.* **56**, 87 (1973).
- ¹⁸M. Szwarc and D. Williams, *Proc. R. Soc. London Ser.* **219**, 353 (1953).
- ¹⁹H. M. Rosenstock, K. Draxl, B. W. Steiner and J. T. Herron, *J. Phys. Chem. Ref. Data* **6**, Suppl. 1 (1977).
- ²⁰D. F. McMillan and D. M. Golden, *Annu. Rev. Phys. Chem.* **33**, 493 (1982).
- ²¹S. W. Benson and H. E. O'Neal, *Kinetic Data on Gas Phase Unimolecular Reactions*, Natl. Stand. Ref. Data Ser., Natl. Bur. Stand. No. 21 (U.S. Dept. of Commerce, Washington, D.C., 1970).
- ²²D. G. L. James and R. D. Stuart, *Trans. Faraday Soc.* **64**, 2752 (1968).
- ²³A. S. Rodgers, D. M. Golden, and S. W. Benson, *J. Am. Chem. Soc.* **89**, 4578 (1967).
- ²⁴S. A. Safron, N. D. Weinstein, D. R. Herschbach, and J. C. Tully, *Chem. Phys. Lett.* **12**, 564 (1972).
- ²⁵RRKM algorithm of W. L. Hase and D. L. Bunker, Quantum Chemistry Program Exchange, University of Indiana, Bloomington, Indiana.
- ²⁶(a) L. M. Sverdlov, M. A. Kovner, and E. P. Krainov, *Vibrational Spectra of Polyatomic Molecules* (Wiley, New York, 1974); (b) A. Amano, O. Horie, and N. H. Hanh, *Int. J. Chem. Kinet.* **8**, 321 (1976).
- ²⁷J. A. Kerr and M. J. Parsonage, *Evaluated Kinetic Data on Gas Phase Addition Reactions* (Chemical Rubber, Cleveland, 1972).
- ²⁸P. J. Robinson and K. A. Holbrook, *Unimolecular Reactions* (Wiley, New York, 1972).
- ²⁹C. S. Parmenter and B. M. Stone, *J. Chem. Phys.* **84**, 4710 (1986).
- ³⁰D. B. Moss, C. S. Parmenter and G. E. Ewing, *J. Chem. Phys.* **86**, 51 (1987).
- ³¹K. Okuyama, N. Mikami and M. Ito, *J. Phys. Chem.* **89**, 5617 (1985).
- ³²See for example, (a) L. Salem, *The Molecular Orbital Theory of Conjugated Systems* (Benjamin, New York, 1966); (b) R. McWeeny, *Coulson's Valence*, 3rd ed. (Oxford University, Oxford, 1979).
- ³³I. Fleming, *Frontier Orbitals and Organic Chemical Reactions* (Wiley, New York, 1978).
- ³⁴G. W. Wheland, *J. Am. Chem. Soc.* **64**, 900 (1942).
- ³⁵J. C. Polanyi and N. Sathyamurthy, *Chem. Phys.* **33**, 287 (1978).
- ³⁶(a) H. Schor, S. Chapman, S. Green, and R. N. Zare, *J. Chem. Phys.* **69**, 3790 (1978); (b) S. Chapman, *ibid.* **74**, 1001 (1981).
- ³⁷D. Krajnovich, L. J. Butler, and Y. T. Lee, *J. Chem. Phys.* **81**, 3031 (1984); T. K. Minton, Ph. D. thesis, University of California, Berkeley, 1986; T. K. Minton, G. M. Nathanson, and Y. T. Lee, *J. Chem. Phys.* **86**, 1991 (1987).
- ³⁸M. J. Krech, S. J. W. Price, and H. J. Sapiiano, *Can. J. Chem.* **55**, 4222 (1977).
- ³⁹J. D. Cox, H. A. Gundry, D. Harrop, and A. J. Head, *J. Chem. Thermodyn.* **1**, 77 (1969).
- ⁴⁰S. W. Benson, F. R. Cruickshank, D. M. Golden, G. R. Haugen, H. E. O'Neal, A. S. Rodgers, R. Shaw, and R. Walsh, *Chem. Rev.* **69**, 279 (1969).
- ⁴¹M. Quack, *Chem. Phys.* **51**, 353 (1980).
- ⁴²C. K. Ingold, *Structure and Mechanism in Organic Chemistry*, 2nd ed. (Cornell University, Ithaca, 1969).
- ⁴³J. S. Yadav, P. C. Mishra, and D. K. Rai, *Mol. Phys.* **26**, 193 (1973).
- ⁴⁴G. N. Robinson, R. E. Continetti, and Y. T. Lee, *J. Chem. Phys.* **89**, 6238 (1988).